International Journal of Civil Engineering and Technology (IJCIET)
Volume 10, Issue 03, March 2019, pp. 349-360, Article ID: IJCIET_10_03_036
Available online at http://www.iaeme.com/ijciet/issues.asp?JType=IJCIET&VType=10&IType=03
ISSN Print: 0976-6308 and ISSN Online: 0976-6316

MODELLING OF CRYSTAL GROWTH IN PEAT SOIL STABILIZED WITH MIXING OF LIME CACO3 AND FLY ASH

Faisal Estu Yulianto
Civil Engineering Lecturer, Engineering Faculty, Madura University, Pamekasan, East Java, 69371.

Basuki Widodo
Professor of Mathematics, Faculty of Mathematics and Natural Sciences
Sepuluh Nopember Institute of Technology, Surabaya
Kampus Sukolilo, Keputih Surabaya, 60111

ABSTRACT

Peat soil stabilization produces improved parameters because of the admixture added to form crystals that fill the pore and wrap the peat soil. Crystal growth is strongly influenced by the filtration of water from its surroundings, the width of area stabilization, and the curing periods. To predict the parameter behaviour of stabilized Peat Soil during the curing periods, the Difference Method is employed by assuming crystal growth occurs in porous media. Control equations are built on the behaviour of peat crystal growth, mass conservation, and Darcy's law. Numerical computing is based on several control statements made and completed with the assistance of Mat Labs software. The prediction of stabilized Peat Soil parameters is modelled in the width of the stabilization area and the different curing periods. Predictive results through numerical computing show that the soil volume, porosity and flow of stabilized peat fluid in the stabilization area of 70 is the most optimal value compared to the width of the other stabilization areas.

Keywords: Peat Soil, Crystal Growth, Computing Simulation.

Cite this Article: Faisal Estu Yulianto and Basuki Widodo, Modelling of Crystal Growth in Peat Soil Stabilized With Mixing of Lime Caco3 and Fly Ash, International Journal of Civil Engineering and Technology, 10(3), 2019, pp. 349-360

http://www.iaeme.com/IJCIET/issues.asp?JType=IJCIET&VType=10&IType=03

1. INTRODUCTION

Peat Soil is organic soils that have very low bearing capacity and high compression ([1]; [2], [3], [4]) therefore, a method of soil improvement is needed as a model for civil buildings. The Peat Soil stabilization method continues to be developed because it is more environmentally friendly and is associated with lower costs ([1], [5]). Stabilization of Peat Soil by mixing Lime sludge and fly ash can increase carrying capacity and reduce compression, which can then support the load better than the initial conditions. This behaviour is caused by CaSiO3 crystals forming ([6]; [7]) to fill the pore and wrap the peat fibre.

Chrysanthemum development is strongly influenced by the concentration of solution (molarity), temperature, energy used in the stages of growth (agitation), and external addition (seeding agent) ([8]). The process of developing and growing peat crystals is also influenced by the curing periods of stabilization where, over time, the growing peat crystals fill the pore and wrap the peat fibre. Based on the growth behaviour of the peat crystals, a mathematical model will be generated to predict its behaviour in stabilized Peat Soil with Lime sludge and fly ash.

2. CRYSTALLIZATION

Crystallization is the development of a specific crystalline solid phase where the surface is in the form of a grid ([9]). This is due to the saturated conditions for a solution and cold conditions for a liquid. Crystallization might be formed through 3 processes, such as the development of a saturated condition in a solution, the development of a crystal nucleus in the solution (nucleation), and the growth of crystal molecules from the nucleation phase until they reach equilibrium state. Crystal growth is also strongly influenced by the concentration of the solution (molarity), temperature, energy used in the growth stages (agitation) and external addition (seeding agent). During the crystallization process there is a change in potential energy ($\Delta\mu$), which is influenced by Boltzmann's constant (k), temperature (T), and the ratio between product activity (AP) and equilibrium constant (K_{eq}), where the magnitude $\Delta\mu$ is obtained from the following equation ([10]):

$$\Delta\mu = kT \ln\left(\frac{AP}{K_{eq}}\right) \quad (1)$$

By using the fluid interaction with solids in porous media, changes in the solids density can be determined by the equation :

$$\frac{\partial \rho_s(1-\phi)}{\partial t} = \Gamma \quad (2)$$

with φ is porosity, ρ_s is the density of solids and Γ is the rate of mass transfer, and

$$\Gamma = \bar{R}A(c - c_{eq}) \quad (3)$$

where c is the concentration at time Δt, $c_{eq} = k_{eq}$ is balanced concentration, $\bar{R}$ is the reaction rate, and A is the surface area, the equation is:

$$\frac{\partial \rho_s}{\partial t} = \frac{\bar{R}A(c-c_{eq})}{(1-\phi)} \quad (4)$$

The crystallization process of Peat Soil is also influenced by the water supply in the peat pore ([11]) hence there is a diffusion process which includes mass transfer of the difference

in solution concentration. The fast-developed crystallization process will cause the crystals to be dissolved (released) again due to water filtration with different concentrations than before ([10]; [12]).

3. MODEL OF PEAT SOIL CRYSTAL GROWTH

The mathematical model will be built from a fluid flow model through porous media developed from crystals and seepage, while the governing equation is used for the development of the two models. A sketch of the peat stabilization model influenced by the water flow on porous media in the laboratory is shown in Figure 1, where the flow affects the growth of peat crystals in the direction of x, y, and z. Based on the occurring crystal growth behavior, some control equations used in the mathematical model are as follows.

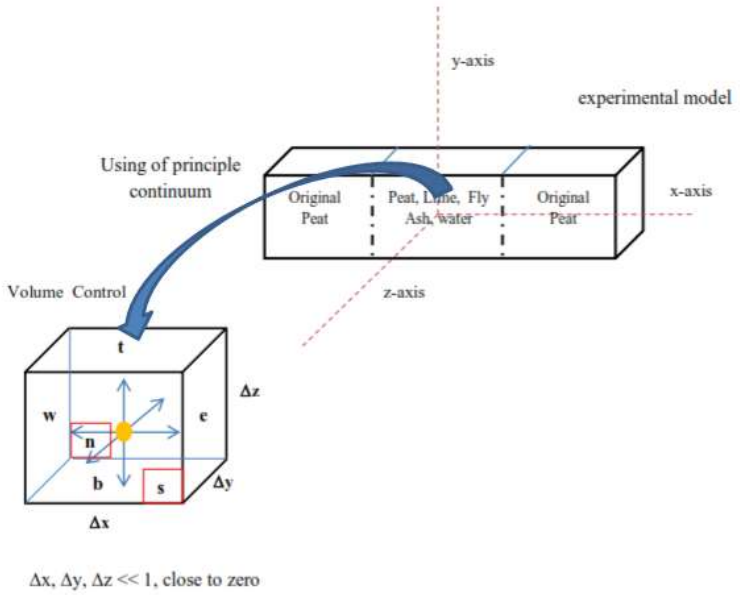

Figure 1. Schematic laboratory model

3.1. Law of Mass Conservation

Addition of admixture to the Peat Soil stabilization will result in the development of $CaSiO_3$ crystals where there is a change in mass from the initial conditions. Apsley ([13]) states that the change in the average mass in the control volume, coupled with the mass flow out through the control surface, is equal to the amount of mass created from the source and expressed in the following equation:

$$\frac{d}{dt}(\text{mass}) + \text{flow out of mass} = \text{Mass source} \tag{5}$$

With ρ as the density of fluid, u as the longitudinal direction of fluid flow, v as the lateral fluid flow rate, w as the vertical fluid flow rate, and ϕ as porosity, the mass conversion equation is written as

$$u\frac{\partial \rho}{\partial x} + \rho\frac{\partial u}{\partial x} + v\frac{\partial \rho}{\partial y} + \rho\frac{\partial v}{\partial y} + w\frac{\partial \rho}{\partial z} + \rho\frac{\partial w}{\partial z} = -\left(\phi\frac{\partial \rho}{\partial t} + \rho\frac{\partial \phi}{\partial t}\right) \tag{6}$$

while the change in porosity to time is obtained by using the following equation :

$$\frac{\partial \phi}{\partial t} + \nabla \mathbf{v}\phi = -\frac{\Gamma}{\rho} \tag{7}$$

Using Darcy's law, the velocity of fluid flow in porous media equation is:

$$v = -\frac{k}{\mu}\frac{\partial P}{\partial x} \tag{8}$$

therefore, the porosity change equation can be written as:

$$\frac{\partial \phi}{\partial t} = -\phi\left(\frac{\partial u}{\partial x} + \frac{\partial v}{\partial y} + \frac{\partial w}{\partial z}\right) - \frac{\bar{R}A(c - c_{eq})}{\rho} \tag{9}$$

then the solid mass growth equation is:

$$\frac{\partial P}{\partial t} = \frac{k}{\phi \mu c_t}\left(\frac{\partial^2 P}{\partial x^2} + \frac{\partial^2 P}{\partial y^2} + \frac{\partial^2 P}{\partial z^2}\right) \tag{10}$$

With $c_t = c_f + c_\phi$, where c_t is a change in compressibility to time, c_ϕ the compressibility of rock development, and c_f is compressibility of fluid.

3.2. Fluid Flow Model in Porous Media

The fluid flow model on porous media can be expressed by the Navier-Stokes equation as follows:

$$\frac{\partial u}{\partial t} + (\mathbf{u} \,.\, \nabla)\left(\frac{\mathbf{u}}{\phi}\right) = -\frac{1}{\rho}\nabla(\phi h) + v_e \nabla^2 \mathbf{u} + \mathbf{F} \tag{11}$$

Because of $\mathbf{F} = -\frac{\phi v}{K}\mathbf{u} - \frac{\phi F_\phi}{\sqrt{K}}|\mathbf{u}|\mathbf{u} + \phi\, G$, and $G = 0$ (12)

where **F** is total body forc, K is permeability, v is shear viscosity, ϕ is porosity, and G is external force, the equation written in the direction of the x-axis is as follows:

$$\frac{\partial u}{\partial t} = -\frac{u}{\phi}\frac{\partial u}{\partial x} - \frac{\phi}{\rho}\frac{\partial P}{\partial x} + v_e \frac{\partial^2 u}{\partial x^2} - \frac{\phi v}{K}u - \frac{\phi F_n}{\sqrt{K}}\left(\sqrt{u^2 + v^2 + w^2}\right)u \tag{13}$$

then the equation written in the direction of the y-axis is:

$$\frac{\partial v}{\partial t} = -\frac{v}{\phi}\frac{\partial v}{\partial y} - \frac{\phi}{\rho}\frac{\partial P}{\partial y} + v_e \frac{\partial^2 v}{\partial y^2} - \frac{\phi v}{K}v - \frac{\phi F_\phi}{\sqrt{K}}\left(\sqrt{u^2 + v^2 + w^2}\right)v \tag{14}$$

then the equation written in the direction of the z-axis is:

$$\frac{\partial w}{\partial t} = -\frac{w}{\phi}\frac{\partial w}{\partial z} - \frac{\phi}{\rho}\frac{\partial P}{\partial z} + v_e \frac{\partial^2 w}{\partial z^2} - \frac{\phi v}{K}w - \frac{\phi F_\phi}{\sqrt{K}}\left(\sqrt{u^2 + v^2 + w^2}\right)w \tag{15}$$

3.3. Non-Dimensional Equation

To simplify matters, non-uniform control questions will be designed into non-dimensional equations. The non-dimensional variables introduced are as follows:

$$\rho = \rho_o \rho^* \tag{16}$$

$$t = \frac{L_0}{U_0}t^* \tag{17}$$

$$u = U_0 u^* \tag{18}$$

$$v = U_0 v^* \tag{19}$$

$$w = U_0 w^* \tag{20}$$

$$x = L_0 x^* \tag{21}$$

$$y = L_0 y^* \tag{22}$$

$$z = L_0 z^* \tag{23}$$

$$\phi = \phi_0 \phi^* \tag{24}$$

$$P = \rho U_0^2 P^* \tag{25}$$

$$Da = \frac{K}{L^2} \tag{26}$$

from equation (6), if the equation is changed into non-dimensional equation, then the equation is:

$$-\rho \frac{\partial u}{\partial x} + u\frac{\partial \rho}{\partial x} - \rho \frac{\partial v}{\partial y} + v\frac{\partial \rho}{\partial y} - \rho \frac{\partial w}{\partial z} + w\frac{\partial \rho}{\partial z} = \phi_0 \phi \frac{\partial \rho}{\partial t} \tag{27}$$

from equation (10) if the equation is changed into non-dimensional equation, then the equation is:

$$\frac{\partial P}{\partial t} = \frac{L_0 k}{\rho_0 U_0 \phi \mu (c_\phi + c_f)} \left(\frac{\partial^2 P}{\partial x^2} + \frac{\partial^2 P}{\partial y^2} + \frac{\partial^2 P}{\partial z^2}\right) \tag{28}$$

from equation (13) if the equation is changed into non-dimensional equation, then the equation is:

$$\frac{\partial u}{\partial t} = -\frac{u}{\phi_0 \phi}\frac{\partial u}{\partial x} - \frac{\phi_0 \phi}{\rho}\frac{\partial P}{\partial x} + v_e \frac{\partial^2 u}{U_0 L_0\, \partial (x)^2} - \frac{\phi_0 \phi v}{K L_0} u$$

$$-\frac{\phi_0 \phi F_\phi L_0}{\sqrt{K}} \left(\sqrt{(u)^2 + (v)^2 + (w)^2}\right) u \tag{29}$$

from equation (14) if the equation is changed into non-dimensional equation, then the equation is:

$$\frac{\partial v}{\partial t} = -\frac{v}{\phi_0 \phi}\frac{\partial v}{\partial y} - \frac{\phi_0 \phi}{\rho}\frac{\partial P}{\partial y} + v_e \frac{\partial^2 v}{U_0 L_0\, \partial (y)^2} - \frac{\phi_0 \phi v}{K L_0} v$$

$$-\frac{\phi_0 \phi F_\phi L_0}{\sqrt{K}} \left(\sqrt{(u)^2 + (v)^2 + (w)^2}\right) v \tag{30}$$

from equation (15) if the equation is changed into non-dimensional equation, then the equation is:

$$\frac{\partial w}{\partial t} = -\frac{w}{\phi_0 \phi}\frac{\partial w}{\partial z} - \frac{\phi_0 \phi}{\rho}\frac{\partial P}{\partial z} + v_e \frac{\partial^2 w}{U_0 L_0\, \partial (z)^2} - \frac{\phi_0 \phi v}{K L_0} w$$

$$-\frac{\phi_0 \phi F_\phi L_0}{\sqrt{K}} \left(\sqrt{(u)^2 + (v)^2 + (w)^2}\right) w \tag{31}$$

3.4. Mac Cormack Method

The Mac Cormack is a discretization method, widely used to solve hyperbolic partial differential equations consisting of two stages of achievement, including the predictor stage and the corrector stage. This method is used because the predictor growth of peat crystals is influenced by growth in the previous time t_{n-1}.

1. Unit Weight of Peat Soil

The Predictor Stage equation (4) is written as:

$$\rho_{s_{i,j,k}}^{\overline{n+1}} = \rho_{s_{i,j,k}}^{n} + \Delta t\left[\frac{RA(c-c_{eq})}{(1-\phi)}\right] \tag{32}$$

The Corrector Stage equation (4) is written as:

$$\rho_{s_{i,j,k}}^{n+1} = 0.5\left[\rho_{s_{i,j,k}}^{n} + \left[\rho_{s_{i,j,k}}^{\overline{n+1}} + \Delta t\left[\frac{RA(c-c_{eq})}{(1-\phi)}\right]\right]\right] \tag{33}$$

2. Void Ratio of Peat Soil

The Predictor Stage equation (9) is written as:

$$\phi_{i,j,k}^{\overline{n+1}} = \phi_{i,j,k}^{n} + \Delta t\left[-\phi_{i,j,k}^{n}\left[\left(\frac{u_{i+1,j,k}^{n}-u_{i,j,k}^{n}}{\Delta x}\right) + \left(\frac{v_{i,j+1,k}^{n}-v_{i,j,k}^{n}}{\Delta y}\right)\right.\right.$$

$$\left.\left. + \left(\frac{w_{i,j,k+1}^{n}-w_{i,j,k}^{n}}{\Delta z}\right)\right] - \left(\frac{RA(c-c_{eq})}{\rho}\right)\right] \tag{34}$$

The Corrector Stage equation (9) is written as:

$$\phi_{i,j,k}^{n+1} = 0.5\left[\phi_{i,j,k}^{n} + \left[\phi_{i,j,k}^{\overline{n+1}} + \Delta t\left[-\phi_{i,j,k}^{\overline{n+1}}\left[\left(\frac{u_{i,j,k}^{n} - u_{i-1,j,k}^{n}}{\Delta x}\right)\right.\right.\right.\right.$$

$$\left.\left.\left.\left. + \left(\frac{v_{i,j,k}^{n}-v_{i,j-1,k}^{n}}{\Delta y}\right) + \left(\frac{w_{i,j,k}^{n}-w_{i,j,k-1}^{n}}{\Delta z}\right)\right] - \left(\frac{RA(c-c_{eq})}{\rho}\right)\right]\right]\right] \tag{35}$$

3.Density of Fluid

The Predictor Stage equation (6) is written as:

$$\rho_{i,j,k}^{\overline{n+1}} = \rho_{i,j,k}^{n} + \frac{\Delta t}{\phi_{i,j,k}^{n}}\left[-\rho_{i,j,k}^{n}\left(\frac{\phi_{i,j,k}^{n+1}-\phi_{i,j,k}^{n}}{\Delta t}\right) - \rho_{i,j,k}^{n}\left(\frac{u_{i+1,j,k}^{n}-u_{i,j,k}^{n}}{\Delta x}\right) + u_{i,j,k}^{n}\left(\frac{\rho_{i+1,j,k}^{n}-\rho_{i,j,k}^{n}}{\Delta x}\right) -\right.$$

$$\rho_{i,j,k}^{n}\left(\frac{v_{i,j+1,k}^{n}-v_{i,j,k}^{n}}{\Delta y}\right) + v_{i,j,k}^{n}\left(\frac{\rho_{i,j+1,k}^{n}-\rho_{i,j,k}^{n}}{\Delta y}\right)$$

$$\left. - \rho_{i,j,k}^{n}\left(\frac{w_{i,j,k+1}^{n}-w_{i,j,k}^{n}}{\Delta z}\right) + w_{i,j,k}^{n}\left(\frac{\rho_{i,j,k+1}^{n}-\rho_{i,j,k}^{n}}{\Delta z}\right)\right] \tag{36}$$

The Corrector Stage equation (6) is written as:

$$\rho_{i,j,k}^{n+1} = 0.5\left[\rho_{i,j,k}^{n} + \left[\rho_{i,j,k}^{\overline{n+1}} + \frac{\Delta t}{\phi_{i,j,k}^{n}}\left[\rho_{i,j,k}^{\overline{n+1}}\left(\frac{2\,\phi_{i,j,k}^{n+1}-\phi_{i,j,k}^{n}+\phi_{i,j,k}^{\overline{n+1}}}{\Delta t}\right)\right.\right.\right.$$

$$\left.\left.\left. - \rho_{i,j,k}^{\overline{n+1}}\left(\frac{u_{i,j,k}^{n}-u_{i-1,j,k}^{n}}{\Delta x}\right) + u_{i,j,k}^{n}\left(\frac{\rho_{i,j,k}^{\overline{n+1}}-\rho_{i-1,j,k}^{\overline{n+1}}}{\Delta x}\right) - \rho_{i,j,k}^{\overline{n+1}}\left(\frac{v_{i,j,k}^{n}-v_{i-1,j,k}^{n}}{\Delta y}\right)\right.\right.\right.$$

$$+v_{i,j,k}^{n}\left(\frac{\rho_{i,j,k}^{\overline{n+1}}-\rho_{i,j-1,k}^{\overline{n+1}}}{\Delta y}\right)-\rho_{i,j,k}^{\overline{n+1}}\left(\frac{w_{i,j,k}^{n}-w_{i,j,k-1}^{n}}{\Delta z}\right)$$

$$+w_{i,j,k}^{n}\left(\frac{\rho_{i,j,k}^{\overline{n+1}}-\rho_{i,j,k-1}^{\overline{n+1}}}{\Delta z}\right)\Bigg]\Bigg]\Bigg] \quad (37)$$

4. Fluid Pressure

The Predictor Stage equation (10) is written as:

$$P_{i,j,k}^{\overline{n+1}}=P_{i,j,k}^{n}+\Delta t\left[\left(\frac{L_0 k}{\rho_0 U_0 \phi\mu\left(c_\phi+c_f\right)}\right)\left(\left(\frac{P_{i+2,j,k}^{n}-2P_{i+1,j,k}^{n}+P_{i,j,k}^{n}}{(\Delta x)^2}\right)\right.\right.$$

$$\left.\left.+\left(\frac{P_{i,j+2,k}^{n}-2P_{i,j+1,k}^{n}+P_{i,j,k}^{n}}{(\Delta y)^2}\right)+\left(\frac{P_{i,j,k+2}^{n}-2P_{i,j,k+1}^{n}+P_{i,j,k}^{n}}{(\Delta z)^2}\right)\right)\right] \quad (38)$$

The Corrector Stage equation (10) is written as:

$$P_{i,j,k}^{n+1}=0.5\left[P_{i,j,k}^{n}+\left[P_{i,j,k}^{\overline{n+1}}+\Delta t\left[\left(\frac{L_0 k}{\rho_0 U_0 \phi\mu\left(c_\phi+c_f\right)}\right)\right.\right.\right.$$

$$\left(\left(\frac{P_{i,j,k}^{\overline{n+1}}-2P_{i-1,j,k}^{\overline{n+1}}+P_{i-2,j,k}^{\overline{n+1}}}{(\Delta x)^2}\right)+\left(\frac{P_{i,j,k}^{\overline{n+1}}-2P_{i,j-1,k}^{\overline{n+1}}+P_{i,j-2,k}^{\overline{n+1}}}{(\Delta y)^2}\right)\right.$$

$$\left.\left.\left.\left.+\left(\frac{P_{i,j,k}^{\overline{n+1}}-2P_{i,j,k-1}^{\overline{n+1}}+P_{i,j,k-2}^{\overline{n+1}}}{(\Delta z)^2}\right)\right)\right]\right]\right] \quad (39)$$

5. Velocity of Fluid in Porous Media for x

The Predictor Stage equation (29) is written as:

$$u_{i,j,k}^{\overline{n+1}}=u_{i,j,k}^{n}+\Delta t\left[-\frac{u_{i,j,k}^{n}}{\phi_0\phi}\left(\frac{u_{i+1,j,k}^{n}-u_{i,j,k}^{n}}{\Delta x}\right)-\frac{\phi_0\phi}{\rho}\left(\frac{P_{i+1,j,k}^{n}-P_{i,j,k}^{n}}{\Delta x}\right)\right.$$

$$+\frac{v_e}{U_0 L_0}\left(\frac{u_{i+2,j,k}^{n}-2u_{i+1,j,k}^{n}+u_{i,j,k}^{n}}{(\Delta x)^2}\right)-\frac{\phi_0\phi v}{KL_0}u_{i,j,k}^{n}-\frac{\phi_0\phi F_\phi L_0}{\sqrt{K}}$$

$$\left.\left(\sqrt{\left(u_{i,j,k}^{n}\right)^2+\left(v_{i,j,k}^{n}\right)^2+\left(w_{i,j,k}^{n}\right)^2}\right)u_{i,j,k}^{n}\right] \quad (40)$$

The Corrector Stage equation (29) is written as:

$$u_{i,j,k}^{n+1}=0.5\left[u_{i,j,k}^{n}+\left[u_{i,j,k}^{\overline{n+1}}+\Delta t\left[-\frac{u_{i,j,k}^{\overline{n+1}}}{\phi_0\phi}\left(\frac{u_{i,j,k}^{\overline{n+1}}-u_{i-1,j,k}^{\overline{n+1}}}{\Delta x}\right)\right.\right.\right.$$

$$\left.\left.\left.-\frac{\phi_0\phi}{\rho}\left(\frac{P_{i,j,k}^{\overline{n+1}}-P_{i-1,j,k}^{\overline{n+1}}}{\Delta x}\right)+\frac{v_e}{U_0 L_0}\left(\frac{u_{i,j,k}^{\overline{n+1}}-2u_{i-1,j,k}^{\overline{n+1}}+u_{i-2,j,k}^{\overline{n+1}}}{(\Delta x)^2}\right)-\frac{\phi_0\phi v}{KL_0}u_{i,j,k}^{\overline{n+1}}\right.\right.\right.$$

$$-\frac{\phi_0\phi F_\phi L_0}{\sqrt{K}}\left(\sqrt{\left(u_{i,j,k}^{\overline{n+1}}\right)^2+\left(v_{i,j,k}^{n}\right)^2+\left(w_{i,j,k}^{n}\right)^2}\right)u_{i,j,k}^{\overline{n+1}}\Bigg]\Bigg] \quad (41)$$

6. Velocity of Fluid in Porous Media for y

The Predictor Stage equation (30) is written as:

$$v_{i,j,k}^{\overline{n+1}} = v_{i,j,k}^{n} + \Delta t\left[-\frac{v_{i,j,k}^{n}}{\phi_0\phi}\left(\frac{v_{i,j+1,k}^{n}-v_{i,j,k}^{n}}{\Delta y}\right)-\frac{\phi_0\phi}{\rho}\left(\frac{P_{i,j+1,k}^{n}-P_{i,j,k}^{n}}{\Delta y}\right)\right.$$

$$+\frac{v_e}{U_0L_0}\left(\frac{v_{i,j+2,k}^{n}-2v_{i,j+1,k}^{n}+v_{i,j,k}^{n}}{(\Delta y)^2}\right)-\frac{\phi_0\phi v}{KL_0}v_{i,j,k}^{n}-\frac{\phi_0\phi F_\phi L_0}{\sqrt{K}}$$

$$\left.\left(\sqrt{\left(u_{i,j,k}^{n}\right)^2+\left(v_{i,j,k}^{n}\right)^2+\left(w_{i,j,k}^{n}\right)^2}\right)v_{i,j,k}^{n}\right] \quad (42)$$

The Corrector Stage equation (30) is written as:

$$v_{i,j,k}^{n+1} = 0.5\left[v_{i,j,k}^{n}+\left[v_{i,j,k}^{\overline{n+1}}+\Delta t\left[-\frac{v_{i,j,k}^{\overline{n+1}}}{\phi_0\phi}\left(\frac{v_{i,j,k}^{\overline{n+1}}-v_{i-1,j,k}^{\overline{n+1}}}{\Delta y}\right)\right.\right.\right.$$

$$-\frac{\phi_0\phi}{\rho}\left(\frac{P_{i,j,k}^{n}-P_{i-1,j,k}^{n}}{\Delta y}\right)+\frac{v_e}{U_0L_0}\left(\frac{v_{i,j,k}^{\overline{n+1}}-2v_{i-1,j,k}^{\overline{n+1}}+v_{i-2,j,k}^{\overline{n+1}}}{(\Delta y)^2}\right)-\frac{\phi_0\phi v}{KL_0}v_{i,j,k}^{\overline{n+1}}$$

$$\left.\left.\left.-\frac{\phi_0\phi F_\phi L_0}{\sqrt{K}}\left(\sqrt{\left(u_{i,j,k}^{n}\right)^2+\left(v_{i,j,k}^{n}\right)^2+\left(w_{i,j,k}^{n}\right)^2}\right)v_{i,j,k}^{\overline{n+1}}\right]\right] \quad (43)$$

7. Velocity of Fluid in Porous Media for z

The Predictor Stage equation (31) is written as:

$$w_{i,j,k}^{\overline{n+1}} = w_{i,j,k}^{n} + \Delta t\left[-\frac{w_{i,j,k}^{n}}{\phi_0\phi}\left(\frac{w_{i,j,k+1}^{n}-w_{i,j,k}^{n}}{\Delta z}\right)-\frac{\phi_0\phi}{\rho}\left(\frac{P_{i,j,k+1}^{n}-P_{i,j,k}^{n}}{\Delta z}\right)\right.$$

$$+\frac{v_e}{U_0L_0}\left(\frac{w_{i,j,k+2}^{n}-2w_{i,j,k+1}^{n}+w_{i,j,k}^{n}}{(\Delta z)^2}\right)-\frac{\phi_0\phi v}{KL_0}w_{i,j,k}^{n}-\frac{\phi_0\phi F_\phi L_0}{\sqrt{K}}$$

$$\left.\left(\sqrt{\left(u_{i,j,k}^{n}\right)^2+\left(v_{i,j,k}^{n}\right)^2+\left(w_{i,j,k}^{n}\right)^2}\right)w_{i,j,k}^{n}\right] \quad (44)$$

The Corrector Stage equation (31) is written as:

$$w_{i,j,k}^{n+1} = 0.5\left[w_{i,j,k}^{n}+\left[w_{i,j,k}^{\overline{n+1}}+\Delta t\left[-\frac{w_{i,j,k}^{\overline{n+1}}}{\phi_0\phi}\left(\frac{w_{i,j,k}^{\overline{n+1}}-w_{i,j,k-1}^{\overline{n+1}}}{\Delta z}\right)\right.\right.\right.$$

$$-\frac{\phi_0\phi}{\rho}\left(\frac{P_{i,j,k}^{n}-P_{i,j,k-1}^{n}}{\Delta z}\right)+\frac{v_e}{U_0L_0}\left(\frac{w_{i,j,k}^{\overline{n+1}}-2w_{i,j,k-1}^{\overline{n+1}}+w_{i,j,k-2}^{\overline{n+1}}}{(\Delta z)^2}\right)$$

$$\left.\left.\left.-\frac{\phi_0\phi v}{KL_0}w_{i,j,k}^{\overline{n+1}}-\frac{\phi_0\phi F_\phi L_0}{\sqrt{K}}\left(\sqrt{\left(u_{i,j,k}^{n}\right)^2+\left(v_{i,j,k}^{n}\right)^2+\left(w_{i,j,k}^{n}\right)^2}\right)w_{i,j,k}^{\overline{n+1}}\right]\right] \quad (45)$$

4. RESULT OF COMPUTING SIMULATION

The results of the Mat Lab simulation are shown in Figure 2 to Figure 5 for the parameters of solid mass (γt), porosity (e), fluid velocity (k) and crystal growth velocity (v_c) for different stabilization areas and curing periods. Figure 2 shows the value of γt for A (the width of the stabilization area) with 90 being the highest value at the beginning of the stabilization age where the water in the peat pore macro is sufficient for crystal formation ([5]). As the curing periods of stabilization becomes longer, the value of γt experience changes due to the decrease of water in the pore macro and the value of γt for A = 90 becomes lower due to the process of fibre decomposition ([4]; [11]).

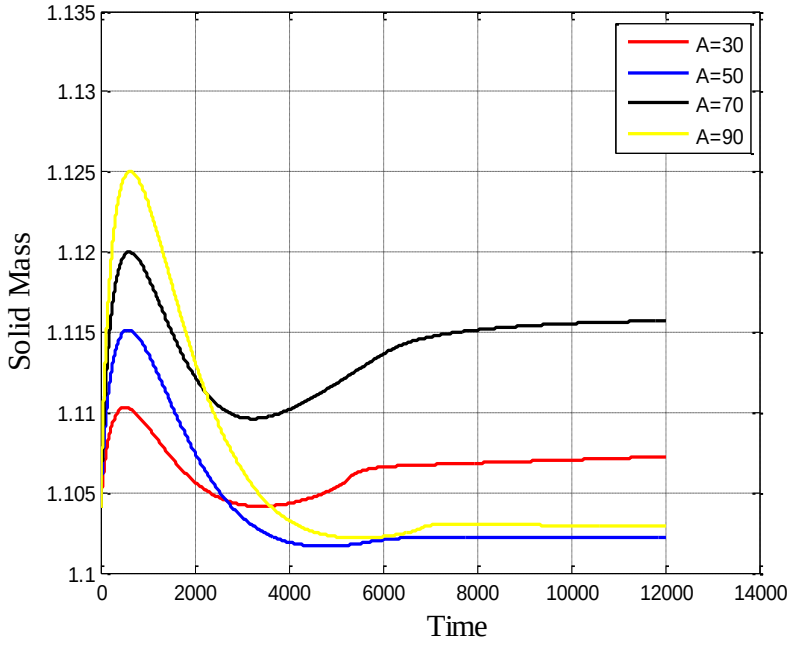

Figure 2. Behavior of solidsmass of stabilized peat

The growth of $CaSiO_3$ crystals on Peat Soil causes its pore (e) to decrease (Figure 3) because of crystals developed through filling Peat Soil pore ([5]; [14]). Figure 3 shows that the largest e value occurs in the stabilization area A = 30 and A = 90; this is due to the growth of crystals at A = 30 which is disturbed by infiltration of water from the surrounding (diffusion) due to the small area of stabilization (A) ([12], [14]). Whereas at A = 90, the value of e becomes large due to the process of crystal decomposition. While the k value difference between variations of the stabilization area width is not much, a decrease of k-value indicates that the crystals are growing with increasing curing periods of stabilization.

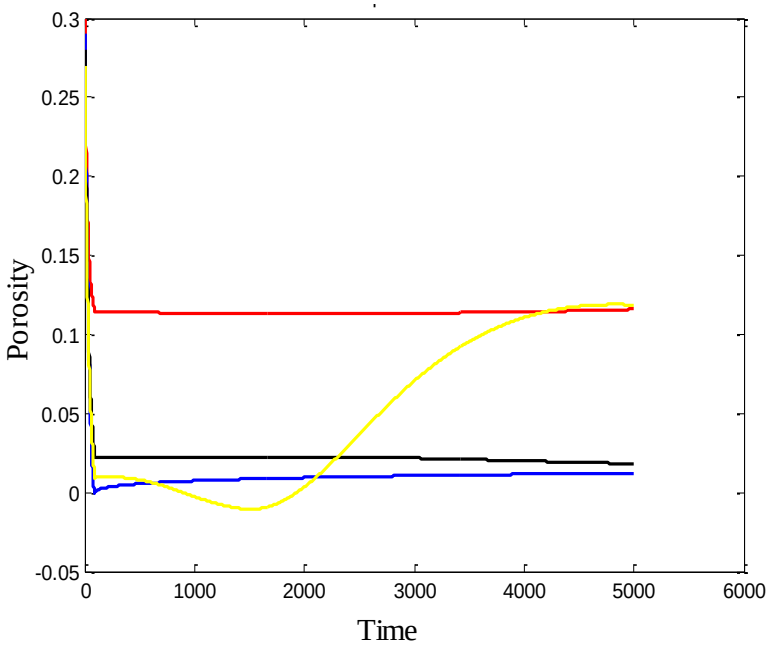

Figure 3. Behavior of Peat stabilized porosity

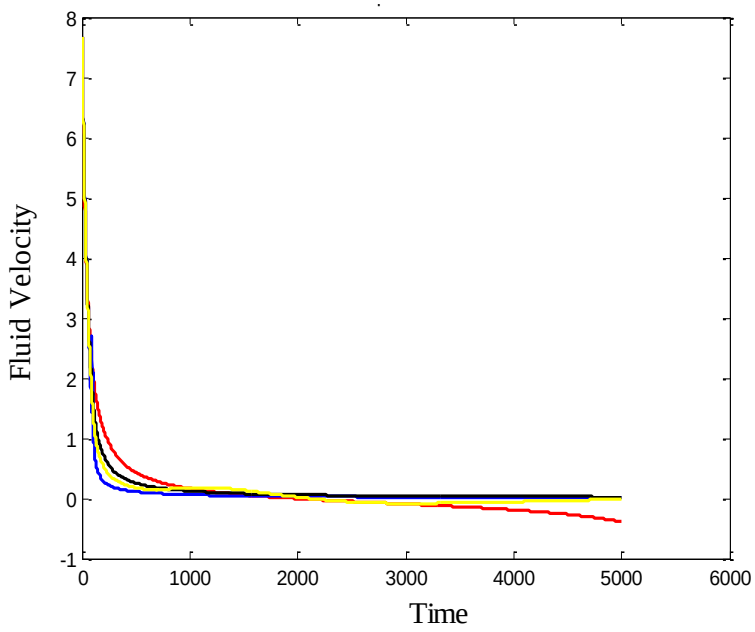

Figure 4. Behavoiur of fluid velocity of stabilized peat

Figure 5 shows the speed of crystal growth decreasing with the increase of curing periods. This behaviour is expected from the value curve γt and e, where the curing periods is below 100. The CaSiO3 crystals growth is rapid and continues to slow when the curing periods increases. This aligns with the research results conducted by Mochtar, N.E., et.al ([5]) and Yulianto and Mochtar, N.E. ([14]).

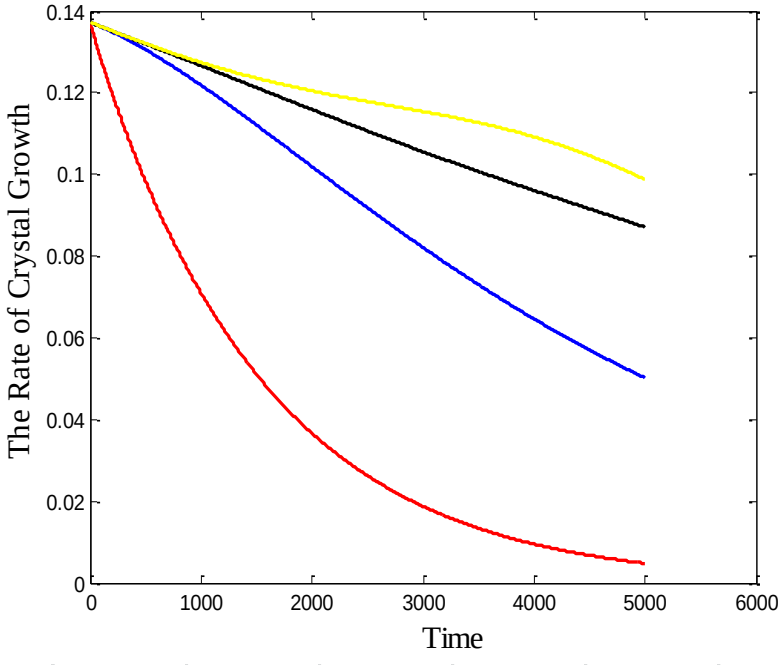

Figure 5. Behavior of rate crystal growth of stabilized peat

This behaviorhas a similar character with solid mass curve and porosity value. When curing periods under 100, crystal growth of $CaSiO_3$ is fastly and became slowly after the time above 100. This is in accordance with the results of research conducted by Mochtar NE., et.all ([5]) andYulianto and Mochtar, NE. ([14])

5. CONCLUSION

Based on the previously described and computer simulations, several points can be concluded, including:

1. Crystal growth is formed quickly at less than 100 and the condition of the peat pore still has enough water to react.
2. Crystal growth in a stabilization width area that is too small (A = 30) or too large (A = 90) causes CaSiO3 crystals to be unstable from the diffusion and decomposition processes.
3. The numerical simulation also show that peat with a stabilization area width (A) 70 produces better parameters due to minimum water filtration.

ACKNOWLEDGEMENTS

Thank you to the Directorate General of Higher Education for the research funding given to us. This publication is part of the research grant. Thank you to all the research teams so that this research can be completed properly.

REFERENCES

[1] Jelisic, N., Leppänen, M., (2001),Mass Stabilization of Peat in Road and Railway construction, Swedish Road Administration, SCC-Viatek Finlandia.

[2] Yulianto, F.E., and Mochtar, N.E. (2010), Mixing of Rice Husk Ash (RHA) and Lime For Peat Stabilization, Proceedings of the First Makassar International Conference on Civil Engineering (MICCE2010), March 9-10, 2010.

[3] Yulianto, F.E., and Mochtar, N.E. (2012), Behaviour of Fibrous Peat Soil Stabilized with Rice Husk Ash (RHA) and Lime, Proceedings of 8th International Symposium on Lowland Technology September 11-13, 2012, Bali, Indonesia.

[4] Yulianto, F.E., Harwadi.,Kusuma W.M., (2014), The Effect of Water Content Reduction to Fibrous Peat Absorbent Capacity and Its Behaviour, Proceedings of 9th International Symposium on Lowland Technology September 29-October 1, 2014, Saga, Japan.

[5] Mochtar, NE, Yulianto, FE., Satria, TR., (2014), Pengaruh Usia Stabilisasi pada Tanah Gambut Berserat yang Distabilisasi dengan Campuran CaCO3 dan Pozolan, Jurnal Teknik Sipil ITB (Civil Engineering Journal ITB), Vol. 21, No. 1, Hal 57-64.

[6] Ingles, O. G., and Metcalf, J. B. (1979), Soil Stabilization (Principles and Practise), Butterworths, Sydney Australia.

[7] Harwadi, F., and Mochtar, N.E. (2010), Compression Behaviour of Peat Soil Stabilized with Environnmentally Friendly Stabilizer, Proceedings of the First Makassar International Conference on Civil Engineering (MICCE2010), March 9-10, 2010).

[8] Mullin, J. W. (1982), Crystallization, Butterworths, London.

[9] Toyukara, Ken et all (1981), Crystallization' in 'Encyclopaedia of Chemical Processing and Design, editor: Mc. Ketta& Cunningham, Marcel Dekker Inc. New York.

[10] Toyukara, Ken et all (1982), Crystallization, Volume I & II, JACE Design Manual Series, Tokyo.

[11] Huttunen, E., and Kujala, K. (1996), On the stabilization of organic soils, In Proceedings of the 2nd International Conference on Ground Improvement Geosystem, IS-Tokyo 96. Vol. 1, pp. 411-414.

[12] Luknanto, Joko (1992), AngkutanLimbah, PAU, IlmuTeknik, Universitas Gajah Mada, Yogyakarta.

[13] Apsley, David (2005), Computational Fluid Dynamic, New York: Spring.

[14] Yulianto, F.E. and Mochtar, N.E. (2016), The Effect Of Curing Period And Thickness Of The Stabilized Peat Layer To The Bearing Capacity And Compression Behavior Of Fibrous Peat, ARPN Journal o Engineering and Applied Science, Vol. 11, No. 19.